

# An Iodide-Based $\text{Li}_7\text{P}_2\text{S}_8\text{I}$ Superionic Conductor

Ezhiylmurugan Rangasamy,<sup>†</sup> Zengcai Liu,<sup>†</sup> Mallory Gobet,<sup>‡</sup> Kartik Pilar,<sup>‡</sup> Gayatri Sahu,<sup>†</sup> Wei Zhou,<sup>§,⊥</sup> Hui Wu,<sup>§,⊥</sup> Steve Greenbaum,<sup>‡</sup> and Chengdu Liang<sup>\*,†</sup>

<sup>†</sup>Center for Nanophase Materials Sciences, Oak Ridge National Laboratory, Oak Ridge, Tennessee 37831, United States

<sup>‡</sup>Department of Physics and Astronomy, Hunter College of the City University of New York, New York, New York 10065, United States

<sup>§</sup>NIST Center for Neutron Research, Gaithersburg, Maryland 20899-6102, United States

<sup>⊥</sup>Department of Materials Science and Engineering, University of Maryland, College Park, Maryland 20742, United States

## Supporting Information

**ABSTRACT:** In an example of stability from instability, a  $\text{Li}_7\text{P}_2\text{S}_8\text{I}$  solid-state Li-ion conductor derived from  $\beta\text{-Li}_3\text{PS}_4$  and LiI demonstrates electrochemical stability up to 10 V vs  $\text{Li}/\text{Li}^+$ . The oxidation instability of I is subverted via its incorporation into the coordinated structure. The inclusion of I also creates stability with the metallic Li anode while simultaneously enhancing the interfacial kinetics and ionic conductivity. Low-temperature membrane processability enables facile fabrication of dense membranes, making this conductor suitable for industrial adoption.

Solid-state electrolytes are quickly rising to prominence as useful components of advanced Li battery technologies due to their excellent electrochemical stability, favorable mechanical properties, and operation over a wide temperature window.<sup>1,2</sup> Previous investigations have resulted in multiple solid-state Li-ion conductors that exhibit favorable characteristics for application in a full electrochemical cell.<sup>1,3</sup> A  $\text{Li}_{10}\text{GeP}_2\text{S}_{12}$  solid-state electrolyte has been reported with conductivity rivaling that of conventional liquid electrolytes.<sup>4</sup> However, the presence of Ge makes it unstable with metallic Li anodes.<sup>5</sup> Despite the number of promising candidates,<sup>1–7</sup> very few systems have been demonstrated to be successful under a full electrochemical setup as a result of interfacial kinetic limitations and electrode–electrolyte compatibility issues.<sup>1</sup>

High-energy batteries use metallic Li as anode and high-voltage materials as cathode. Therefore, it is critical to develop suitable solid electrolytes with high ionic conductivity and excellent chemical stability not only against the Li anode but also at higher voltages, to facilitate high-voltage cathodes and guard against cell abuse. While  $\beta\text{-Li}_3\text{PS}_4$  and its composite Li-ion conductors have been reported to demonstrate the requisite characteristics,<sup>3,6,7</sup> it forms a buffer layer with Li anode to give the observed stability.<sup>8</sup> Further improvements in conductivity, materials processability, and interfacial kinetics are also desired. Typically, sulfide-based ceramic electrolytes demonstrate ionic conductivity on the order of  $10^{-3} \text{ S cm}^{-1}$  when synthesized in the form of solid solutions.<sup>4,5,9–11</sup> However, the presence of electroactive substituents compromises the stability with Li anodes for these high-conduction systems.<sup>5,11</sup> The use of non-electroactive species—alkali halides—has been reported to

enhance ionic conductivity in Ag-based systems.<sup>12</sup> Lithium halides,  $\text{LiX}$  ( $\text{X} = \text{I}, \text{Cl}, \text{and Br}$ ), have been effectively utilized to stabilize the higher conduction phase in the  $\text{LiBH}_4$  system while demonstrating excellent stability with metallic Li.<sup>13,14</sup>  $\text{LiX}$ -based  $\text{Li}_6\text{PS}_5\text{I}$  and other halide derivatives have been developed with an argyrodite structure, with some systems demonstrating fast ion conduction.<sup>15–18</sup> However, there is a lack of detailed investigations on their electrochemical stabilities and interfacial compatibilities. The  $\text{Li}_2\text{S}$ – $\text{P}_2\text{S}_5$  glassy phases have also been reported to form new conduction systems with alkaline halides.<sup>19–21</sup> On account of the oxidation of the alkaline halides, these systems exhibit electrochemical instability in cyclic voltammetry investigations. In addition to that, the onset of reduction occurs before 0 V vs  $\text{Li}/\text{Li}^+$ , suggesting that the electrolyte is not inherently stable with the Li anode. The authors hypothesize that the lack of formation of a new phase with high purity results in manifesting instabilities of the parent precursors with the newly formed systems.

Recently, LiF has been demonstrated to have an effect on the electrochemical properties of  $\beta\text{-Li}_3\text{PS}_4$  (LPS).<sup>22</sup> This creates an interesting scientific problem about the possibility of investigating alkali halide interactions with  $\text{Li}_3\text{PS}_4$  and their effects in comparison with those of other sulfide Li-ion conductors. On account of the variation in unit cell volume and anionic polarizability, a favorable trend in ionic conductivity and activation energy is observed, moving down the periodic table ( $\sigma_{\text{LiI}} > \sigma_{\text{LiBr}} > \sigma_{\text{LiCl}} > \sigma_{\text{LiF}}$ ).<sup>23</sup> Hence, LiI will be an ideal candidate to investigate such interactions. *Is it possible to incorporate LiI into a solid-state Li-ion conductor while simultaneously eliminating the inherent oxidation of LiI and its low ionic conductivity?* Herein we demonstrate that, with the appropriate compositions of LiI and  $\text{Li}_3\text{PS}_4$ , the new phase formed exhibits an electrochemical stability of 10 V vs  $\text{Li}/\text{Li}^+$  while its room-temperature ionic conductivity is simultaneously enhanced to  $6.3 \times 10^{-4} \text{ S cm}^{-1}$  (Figure 1b), 400% higher than that of  $\beta\text{-Li}_3\text{PS}_4$  and more than 3 orders of magnitude higher than that of LiI.<sup>7,24</sup> More importantly, the new phase has a remarkable compatibility with metallic Li anode.

**A New Stoichiometric Phase Is Formed.** Upon mixing LiI with  $\text{Li}_3\text{PS}_4$  and subsequent heat treatment, a new phase

Received: August 24, 2014

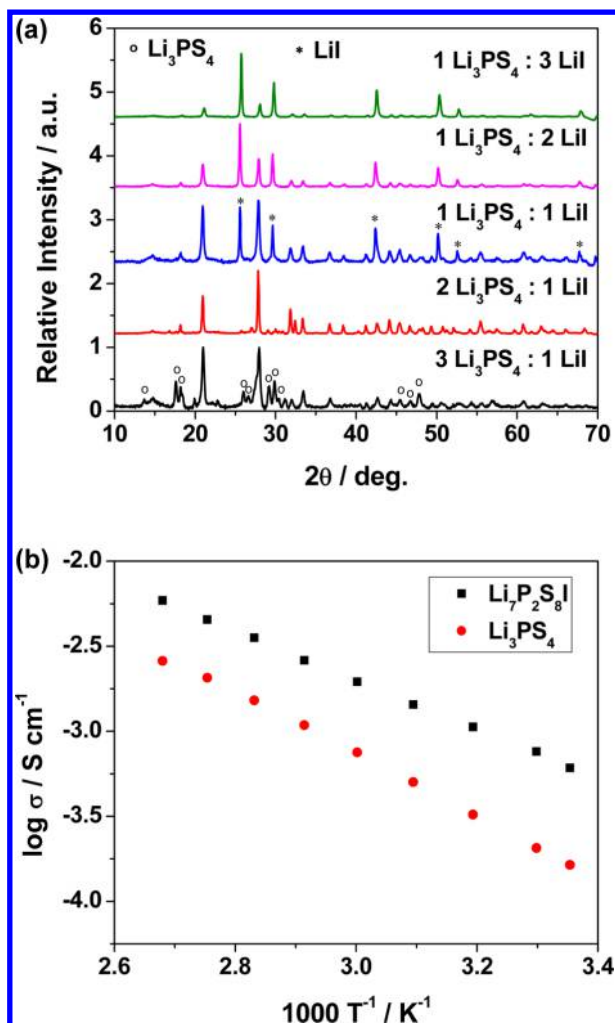
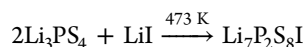


**Figure 1.** (a) XRD data illustrating the formation of a new phase at the 2:1 stoichiometric composition of LPS:LiI. An excess of either phase leads to the observation of the respective phase as a secondary impurity in addition to the newly formed phase. (b) Arrhenius plot of the new phase, demonstrating the 400% increase in ionic conductivity and lower activation energy for the new phase in comparison with  $\text{Li}_3\text{PS}_4$ .

was observed to be formed that was completely different from the parent phases (Figure 1). To investigate this new phase and to elucidate the right chemistry, various stoichiometric compositions of LPS and LiI were mixed and heat-treated at 200 °C. The maximum phase purity was observed at a 2:1 ratio of  $\text{Li}_3\text{PS}_4$ :LiI precursors, with no observed reflections from the parent systems. The presence of an excess of either of the precursors resulted in precipitation of the respective phase in addition to the newly formed phase. A Le Bail refinement (Figure S1) of the 2:1 composition revealed a single phase indexed to a  $Pnma$  space group, similar to the  $\beta$ - $\text{Li}_3\text{PS}_4$ . The excellent fit confirms that it is a singular phase formed as a result of the following reaction:



When the resultant phase was dispersed in acetonitrile (Figure S2) and subsequently dried at 80 °C, LiI dissolved in the solvent and was lost during the solvent removal. XRD analysis of the powders showed the presence of  $\text{Li}_3\text{PS}_4 \cdot 2\text{ACN}$  and partial presence of crystalline  $\text{Li}_3\text{PS}_4$  along with an unknown

phase. With the similarity in the crystal structures and the ability to extract LiI from the  $\text{Li}_7\text{P}_2\text{S}_8\text{I}$ , this newly formed phase is attributed to a solid solution of LiI in  $\text{Li}_3\text{PS}_4$ .

The newly formed phase exhibits an ionic conductivity of  $6.3 \times 10^{-4} \text{ S cm}^{-1}$  at room temperature, a 400% improvement over the ionic conductivity of LPS and more than 3 orders of magnitude over that LiI.<sup>7,24</sup> It has been reported that the introduction of halide ion results in pathways of higher free volume, directly resulting in fast ion conduction properties for the respective systems.<sup>25</sup> This halide effect has significantly enhanced the ionic conductivity of the parent systems. A similar effect could be attributed to the enhancement in ionic conductivity for LiI-reacted samples. It is to be noted that the crystallographic reflection for  $\text{Li}_7\text{P}_2\text{S}_8\text{I}$  is distinctly different from those reported for the  $\text{Li}_6\text{PS}_5\text{X}$  phases, suggesting the presence of a new crystal structure.<sup>15,16,18</sup>

NMR spectroscopic characterization of the newly synthesized phase confirmed the formation of new chemical sites. The  $^{31}\text{P}$  NMR spectrum (Figure 2) revealed two major distinct

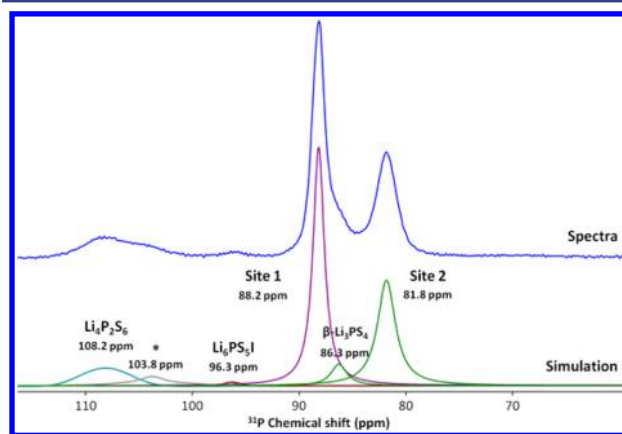


**Figure 2.**  $^{31}\text{P}$  MAS (20 kHz) NMR spectra for the  $\text{Li}_7\text{P}_2\text{S}_8\text{I}$  phase. Two coordination sites are observed for  $\text{PS}_4^{3-}$  tetrahedra. While XRD does not detect the presence of secondary phases, owing to its high resolution, NMR shows the presence of residual  $\beta$ - $\text{Li}_3\text{PS}_4$  and additional secondary phases (\* denotes an unknown phase).

peaks in the chemical shift range of isolated  $\text{PS}_4^{3-}$  tetrahedra, supporting the presence of two coordination sites in  $\text{Li}_7\text{P}_2\text{S}_8\text{I}$ , one conforming to  $\gamma$ - $\text{Li}_3\text{PS}_4$  (88.2 ppm) and the second attributed to a  $\text{PS}_4^{3-}$  tetrahedron with I atoms in the secondary coordination shell (81.8 ppm). Very minor residual  $\beta$ - $\text{Li}_3\text{PS}_4$ <sup>26</sup> is also observed in the NMR, in addition to  $\text{Li}_4\text{P}_2\text{S}_6$ ,<sup>27</sup>  $\text{Li}_6\text{PS}_5\text{I}$ ,<sup>18</sup> and an unknown phase. Detailed structural and spectroscopic characterizations are currently underway to identify the crystal structure and mechanism for fast ion conduction within the newly formed  $\text{Li}_7\text{P}_2\text{S}_8\text{I}$  phase.

Dramatic reactions as a result of overcharging in conventional Li-ion cells are well documented.<sup>28–30</sup> The surge in cell temperature resulting from the cathodic reactions has also been proposed to result in chemical reactions at the anode that complicate cell safety under such conditions. Hence, anodic stability coupled with cathodic stability (i.e., electrochemical stability of the electrolyte), high ionic conductivity, increased temperature stability, and lack of flammability is identified as a vital criterion for next-generation Li-ion cells.<sup>30</sup> Cyclic voltammetry investigation of the  $\text{Li}_7\text{P}_2\text{S}_8\text{I}$  electrolyte (Figure 3a) exhibited electrochemical stability of up to 10 V vs  $\text{Li}/\text{Li}^+$  under the measured conditions. The observed electrochemical

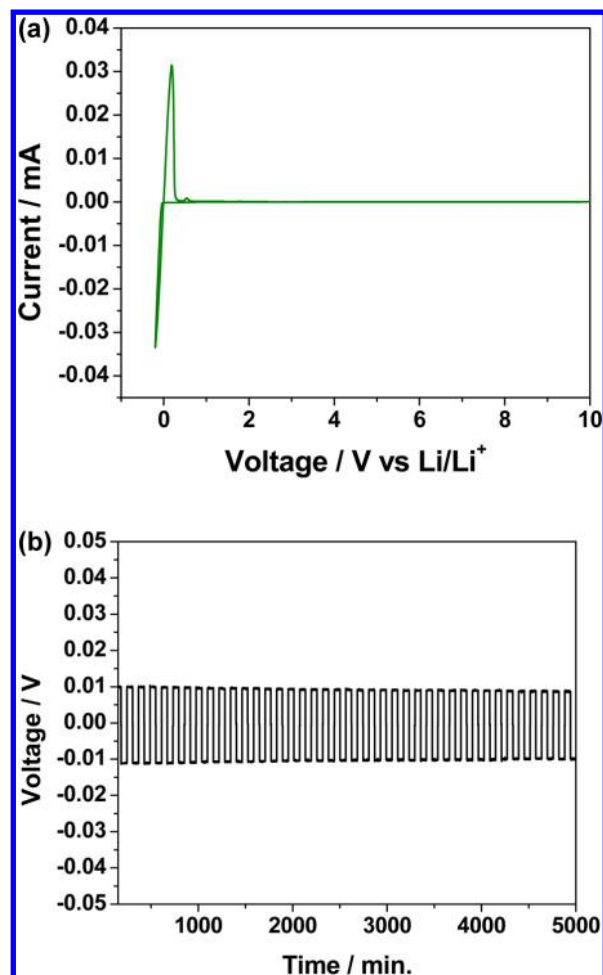


**Figure 3.** (a) Cyclic voltammogram for a Li/Li<sub>7</sub>P<sub>2</sub>S<sub>8</sub>I/Pt cell at a scan rate of 1 mV s<sup>-1</sup>, demonstrating that the new electrolyte phase is stable up to 10 V vs Li/Li<sup>+</sup>. (b) DC polarization curve for a Li/Li<sub>7</sub>P<sub>2</sub>S<sub>8</sub>I/Li symmetric cell at a current density of 0.2 mA cm<sup>-2</sup>, illustrating excellent full-cell conductivity.

stability is higher than that of the state-of-the-art garnet electrolytes (9 V vs Li/Li<sup>+</sup>) and typical sulfide electrolytes (5 V vs Li/Li<sup>+</sup>)<sup>1,3,7,31,32</sup> and on par (10 V vs Li/Li<sup>+</sup>) with an earlier report on oxysulfide glasses.<sup>33</sup> The multiple minor oxidation peaks observed between 0.42 and 0.7 V are attributed to the anodic reactions forming the Pt–Li alloy at the Pt working electrode.<sup>34</sup> The stability of the newly synthesized phase at the oxidative potentials is attributed to the coordination of I within the structure. This result differs from earlier reports with Li<sub>2</sub>S–P<sub>2</sub>S<sub>5</sub>–LiI systems that exhibit minor oxidation of LiI and reduction prior to 0 V.<sup>19,21</sup> The presence of a high-purity Li<sub>7</sub>P<sub>2</sub>S<sub>8</sub>I phase thus eliminates the instabilities of Li<sub>3</sub>PS<sub>4</sub> and LiI.

A control sample prepared with excess LiI (Figure S3a) illustrated that the excess LiI undergoes oxidation at 3.2 V vs Li/Li<sup>+</sup>. This is in contrast to the electrochemical stability of the newly formed phase. It is also critical to closely observe (Figure S3b) the reduction and oxidation of Li. The cathodic reaction occurs only beyond 0 V vs Li/Li<sup>+</sup>. Systems that are typically electroactive with metallic Li or form passive interfaces exhibit onset of a cathodic current before 0 V.<sup>4,11</sup> This confirms the stability for the electrolyte with Li anode.

Symmetric Li/Li<sub>7</sub>P<sub>2</sub>S<sub>8</sub>I/Li cells were fabricated and cycled at ambient conditions (Figure 3b), exhibiting polarization significantly lower than that of the LPS electrolyte or its

composites.<sup>6,7</sup> Calculating DC cell conductivity from the polarization yields a value of  $5.8 \times 10^{-4}$  S cm<sup>-1</sup>, similar to the AC measurement of  $6.3 \times 10^{-4}$  S cm<sup>-1</sup> under a blocking configuration. The lack of difference between total cell conductivity and bulk electrolyte conductivity is a testament to the low charge-transfer resistance (Figure S4). Due to the nature of cell assembly (physically attached Li electrodes), the interfacial resistance reduces with cycling until a homogeneous Li layer is formed. The polarization remains constant after the formation cycles, wherein cycle numbers 30, 100, 400, and 800 overlap one another (Figure S5). The cell has been currently cycled over 800 times, demonstrating an excellent Li cycle life.

**Li<sub>7</sub>P<sub>2</sub>S<sub>8</sub>I Facilitates Membrane Densification via Warm Pressing.** Since Li-ion conduction in a ceramic electrolyte happens in the solid phase, it is quintessential that the membrane be devoid of any pores/voids. One of the major drawbacks of the oxide-based Li-ion conductors is the requirement of high temperatures (>1000 °C) for the densification of membranes.<sup>1</sup> Thus, membrane processability at ambient temperatures or relatively warm temperatures (<300 °C) is critical. The membranes are pressed at 320 MPa and 270 °C, resulting in dense electrolyte membranes with no observed porosity (Figure 4). Earlier reports have demonstrated similar

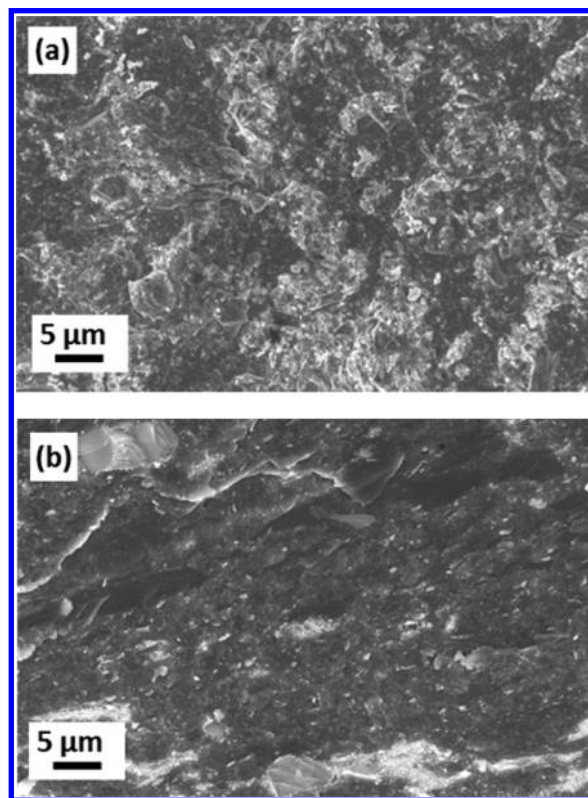


**Figure 4.** SEM images of (a) surface and (b) cross section of a warm pressed Li<sub>7</sub>P<sub>2</sub>S<sub>8</sub>I membrane, showing a highly dense network with no observed voids.

densification with the glassy sulfides.<sup>35,36</sup> The fracturing morphology confirms the occurrence of densification via sintering (Figure S6). Such a low-temperature-based densification enables the possibility of membrane reinforcement using stable polymeric additives. This could be the key to obtaining flexible solid-state Li-ion conductors that are suitable for industrial-scale processing.



To summarize, we have synthesized a new  $\text{Li}_7\text{P}_2\text{S}_8\text{I}$  phase that exhibits the characteristics of a solid solution between  $\text{Li}_3\text{PS}_4$  and  $\text{LiI}$  with fast ion conduction and electrochemical stability up to 10 V vs  $\text{Li}/\text{Li}^+$ . The presence of I enhances the stability of the electrolyte with metallic Li anode while demonstrating low charge-transfer resistance. These characteristics form a foundation that allows the electrolyte to exhibit excellent cycle life and stability at ambient conditions. The material property of the electrolyte allows low-temperature densification and enhanced processability, which is vital to developing industrial-scale solid electrolyte membranes. Currently investigations are underway to identify the crystal structure and mechanism of Li-ion conduction in the newly formed phase along with polymeric reinforcement for flexible solid electrolyte membranes. This opens new avenues for the development of inherently safe all-solid Li batteries.

## ■ ASSOCIATED CONTENT

### ■ Supporting Information

Experimental details and additional data. This material is available free of charge via the Internet at <http://pubs.acs.org>.

## ■ AUTHOR INFORMATION

### Corresponding Author

\*liangcn@ornl.gov

### Notes

The authors declare no competing financial interest.

## ■ ACKNOWLEDGMENTS

This work was sponsored by the Division of Materials Sciences and Engineering, Office of Basic Energy Sciences, U.S. Department of Energy (DOE). The NMR measurements were supported by the DOE BES Division of Materials Chemistry under award DE-SC0005029. The synthesis and characterization of materials were conducted at the Center for Nanophase Materials Sciences, which is sponsored at Oak Ridge National Laboratory by the Division of Scientific User Facilities, U.S. DOE.

## ■ REFERENCES

- (1) Knauth, P. *Solid State Ionics* **2009**, 180, 911.
- (2) Thangadurai, V.; Narayanan, S.; Pinzar, D. *Chem. Soc. Rev.* **2014**, 43, 4714.
- (3) Takada, K. *Acta Mater.* **2013**, 61, 759.
- (4) Kamaya, N.; Homma, K.; Yamakawa, Y.; Hirayama, M.; Kanno, R.; Yonemura, M.; Kamiyama, T.; Kato, Y.; Hama, S.; Kawamoto, K.; Mitsui, A. *Nat. Mater.* **2011**, 10, 682.
- (5) Mo, Y. F.; Ong, S. P.; Ceder, G. *Chem. Mater.* **2012**, 24, 15.
- (6) Rangasamy, E.; Sahu, G.; Keum, J. K.; Rondinone, A. J.; Dudney, N. J.; Liang, C. J. *Mater. Chem. A* **2014**, 2, 4111.
- (7) Liu, Z.; Fu, W.; Payzant, E. A.; Yu, X.; Wu, Z.; Dudney, N. J.; Kiggans, J.; Hong, K.; Rondinone, A. J.; Liang, C. J. *Am. Chem. Soc.* **2013**, 135, 975.
- (8) Lepley, N. D.; Holzwarth, N. A. W.; Du, Y. A. *Phys. Rev. B* **2013**, 88, 104103.
- (9) Kanno, R.; Maruyama, M. *J. Electrochem. Soc.* **2001**, 148, A742.
- (10) Sahu, G.; Lin, Z.; Li, J. C.; Liu, Z. C.; Dudney, N.; Liang, C. D. *Energy Environ. Sci.* **2014**, 7, 1053.
- (11) Sahu, G.; Rangasamy, E.; Li, J.; Chen, Y.; An, K.; Dudney, N.; Liang, C. J. *Mater. Chem. A* **2014**, 2, 10396.
- (12) Maier, J. *Nat. Mater.* **2005**, 4, 805.
- (13) Arnbjerg, L. M.; Ravnsbæk, D. B.; Filinchuk, Y.; Vang, R. T.; Cerenius, Y.; Besenbacher, F.; Jørgensen, J.-E.; Jakobsen, H. J.; Jensen, T. R. *Chem. Mater.* **2009**, 21, 5772.
- (14) Maekawa, H.; Matsuo, M.; Takamura, H.; Ando, M.; Noda, Y.; Karahashi, T.; Orimo, S.-i. *J. Am. Chem. Soc.* **2009**, 131, 894.
- (15) Rayavarapu, P.; Sharma, N.; Peterson, V.; Adams, S. J. *Solid State Electron.* **2012**, 16, 1807.
- (16) Boulineau, S.; Courty, M.; Tarascon, J.-M.; Viallet, V. *Solid State Ionics* **2012**, 221, 1.
- (17) Pecher, O.; Kong, S.-T.; Goebel, T.; Nickel, V.; Weichert, K.; Reiner, C.; Deiseroth, H.-J.; Maier, J.; Haarmann, F.; Zahn, D. *Chem.—Eur. J.* **2010**, 16, 8347.
- (18) Deiseroth, H.-J.; Kong, S.-T.; Eckert, H.; Vannahme, J.; Reiner, C.; Zaiß, T.; Schlosser, M. *Angew. Chem., Int. Ed.* **2008**, 47, 755.
- (19) Ujiie, S.; Hayashi, A.; Tatsumisago, M. *J. Solid State Electron.* **2013**, 17, 675.
- (20) Ujiie, S.; Hayashi, A.; Tatsumisago, M. *Mater. Renew. Sustain. Energy* **2013**, 3, 1.
- (21) Ujiie, S.; Hayashi, A.; Tatsumisago, M. *Solid State Ionics* **2012**, 211, 42.
- (22) Rangasamy, E.; Li, J.; Sahu, G.; Dudney, N.; Liang, C. J. *Am. Chem. Soc.* **2014**, 136, 6874.
- (23) Mercier, R.; Malugani, J. P.; Fahys, B.; Robert, G. *Solid State Ionics* **1981**, 5, 663.
- (24) Liang, C. C. J. *Electrochem. Soc.* **1973**, 120, 1289.
- (25) Sidebottom, D. L. *Phys. Rev. Lett.* **1999**, 83, 983.
- (26) Gobet, M.; Greenbaum, S.; Sahu, G.; Liang, C. *Chem. Mater.* **2014**, 26, 3558.
- (27) Eckert, H.; Zhang, Z.; Kennedy, J. H. *Chem. Mater.* **1990**, 2, 273.
- (28) Leising, R. A.; Palazzo, M. J.; Takeuchi, E. S.; Takeuchi, K. J. *J. Power Sources* **2001**, 97–98, 681.
- (29) Leising, R. A.; Palazzo, M. J.; Takeuchi, E. S.; Takeuchi, K. J. *J. Electrochem. Soc.* **2001**, 148, A838.
- (30) Aurbach, D.; Talyosef, Y.; Markovsky, B.; Markevich, E.; Zinigrad, E.; Asraf, L.; Gnanaraj, J. S.; Kim, H.-J. *Electrochim. Acta* **2004**, 50, 247.
- (31) Ohta, S.; Kobayashi, T.; Asaoka, T. *J. Power Sources* **2011**, 196, 3342.
- (32) Mizuno, F.; Hayashi, A.; Tadanaga, K.; Tatsumisago, M. *Adv. Mater.* **2005**, 17, 918.
- (33) Takada, K.; Aotani, N.; Iwamoto, K.; Kondo, S. *Solid State Ionics* **1996**, 86–88 (Part 2), 877.
- (34) Zhang, S. S.; Xu, K.; Read, J. J. *J. Power Sources* **2011**, 196, 3906.
- (35) Kitaura, H.; Hayashi, A.; Ohtomo, T.; Hama, S.; Tatsumisago, M. *J. Mater. Chem.* **2011**, 21, 118.
- (36) Seino, Y.; Ota, T.; Takada, K.; Hayashi, A.; Tatsumisago, M. *Energy Environ. Sci.* **2014**, 7, 627.